geotechnics

MDPI

Review

A Review of Particle Packing Models and Their Applications to Characterize Properties of Sand-Silt Mixtures

Ching S. Chang * and Jason Chao

Department of Civil and Environmental Engineering, University of Massachusetts, Amherst, MA 01003, USA; jasonchao@umass.edu

* Correspondence: cchang@umass.edu

Abstract: This paper reviews particle packing models and explores their application in geotechnical engineering, specifically for sand-silt mixtures. The review covers key models, including limiting case, linear, and non-linear packing models, focusing on their mathematical structures, physical principles, assumptions, and limitations through the concept of excess free volume. The application of particle packing models in geotechnical engineering is explored in characterizing the properties of sand-silt mixtures, offering insights into maximum, minimum, and critical void ratios and inter-granular void ratio, and the prediction of mechanical properties.

Keywords: particle packing models; sand-silt mixtures; granular potential; void ratio; mechanical behavior; relative density

check for updates

Citation: Chang, C.S.; Chao, J. A Review of Particle Packing Models and Their Applications to Characterize Properties of Sand-Silt Mixtures. *Geotechnics* **2024**, *4*, 1124–1139. https://doi.org/10.3390/geotechnics4040057

Academic Editor: Salvatore Grasso

Received: 7 September 2024
Revised: 3 October 2024
Accepted: 29 October 2024
Published: 1 November 2024

1. Introduction

The study of particle packing volume is important across many fields, including concrete performance [1,2], powder technology [3], ceramics manufacturing [4], and pharmaceuticals [5]. In geotechnical engineering, packing density plays a crucial role in determining soil properties and the performance of granular materials. Understanding the packing density of soil mixtures is essential for many engineering decisions [6,7], such as foundation design and slope stability assessments. Therefore, the particle packing model is potentially valuable in this context.

This paper reviews advances in particle packing models, with a focus on binary mixtures of soil particles ranging in size from 10 μm (silt) to 10,000 μm (sand and coarse aggregates). The review excludes cohesive clay particles, because clay behaves differently from sand and silt due to hydration, plasticity, and long-range inter-particle forces, which require alternative modeling approaches.

We begin by outlining the theoretical background of packing density models, describing the volume change from mixing two particle species based on granular physics. This change is viewed as the sum of the "excess free volume" of each species, arising from their geometric interactions. We then review various models, examining their mathematical structures, physical principles, assumptions, and limitations through the concept of "excess free volume". Finally, the application of these models in geotechnical engineering is explored in three areas: (1) estimating maximum, minimum, and critical state void ratios, (2) establishing connection to the inter-granular void ratio, and (3) predicting relative densities and mechanical properties of soil mixtures.

2. Background

The underlying physics of volume change, due to the mixing of particles of different sizes, can be understood as changes in "granular potential". The framework of Edwards thermodynamics has been applied to study this phenomenon [8], using the following fundamental equation:

$$dv = \chi dS + \sum_{1}^{N} \hat{\mu}_i dy_i \tag{1}$$

Here, v is the specific volume, y_i is the solid fraction of particles, and $\hat{\mu}_i$ is the granular potential for the i-th species. χ is compactivity, and S is the configurational entropy of the packing. Note that the erm χdS is analogous to heat in traditional thermodynamics, while the second term resembles chemical potential [9]. In Edwards thermodynamics, compactivity indicates how easily the packing can be compacted, often referred to as granular temperature.

The granular potential in this context can be understood as Gibbs excess free volume potential or "excess free volume". For a bi-dispersed packing, where particle sizes are denoted by d_1 and d_2, the solid fractions are denoted by y_1 and y_2 for large and small particles, respectively. The total specific volume of the mixture is as follows:

$$v = v_1 y_1 + v_2 y_2 \tag{2}$$

Here, v_i represents the partial volume of the i-th species, analogous to partial mole energy in thermodynamics [9].

For a mono-dispersed packing made of the i-th component of the bi-dispersed mixture, compacted to the same state of χ as the mixture, the volume of the mono-dispersed packing is denoted by v_i^0. The difference between v_i and v_i^0 is

$$\Delta v_i = v_i - v_i^0 \tag{3}$$

This difference (Δv_i) is referred to as the excess free volume of the i-th species, similar to excess free energy in thermodynamics [9]. In this context, "free" refers to the available void space that can be reduced through particle rearrangement. When particles of different sizes mix, small particles fill the voids between large particles, and large particles embed into the matrix of small particles, thereby reducing the overall void space. Therefore, granular potential is essentially the excess free volume, influenced by the particle size ratio and particle shapes of the two species [10].

The excess free volume, denoted as granular potential $\hat{\mu}_i = \Delta v_i$, allows us to express the change in volume (dv) due to bi-dispersity as the sum of two contributions:

$$dv = \chi dS + \sum_{i=1}^{2} \Delta v_i dy_i \; ; \;\; \text{where} \;\; \chi dS = \sum_{i=1}^{2} v_i^0 dy_i \tag{4}$$

In this expression, y_1 represents the solid volume fraction for large particles, and y_2 represents the same for small particles. Since $y_2 = 1 - y_1$, the composition of the bi-dispersed packing can be simplified to the fines content, denoted as $f_c = y_2$.

It is important to note that "excess free volume" is not an intrinsic property of any individual particle species. Rather, it depends on the characteristics of the bi-dispersed mixtures, such as the particle size ratios and the solid fraction of each species.

To calculate the excess free volume, we must first determine the value of v_i (as in Equation (3)). This can be done by using the "add-a-particle" method [8], where adding a particle of i-th species into the packing increases the total packing volume. The ratio of this increase in volume to the solid volume of the added particle gives v_i, which indicates how much space the particles occupy relative to the voids—a key factor in understanding the behavior of soil mixtures.

Figure 1 illustrates four different scenarios for mixtures with very small particle ratios.

(a) When a large particle is added to a uniform packing of large particles, it occupies a space, which includes not only the solid volume of this particle but also the adjacent void volume. The space is similar to the space occupied by a neighboring particle. Thus, the ratio of this increase in volume to the solid volume of the added particle v_1 is equal to v_1^0, meaning the excess free volume $\Delta v_1 = 0$.

(b) Conversely, if a large particle is added to a uniform packing of very small particles, it becomes embedded in the matrix of the small particles. In this scenario, the space occupied by the large particle consists solely of its solid volume, with virtually no adjacent void space. Thus, the ratio of this increase in volume to the solid volume of the added particle v_1 equals 1, and the excess free volume $\Delta v_1 = 1 - v_1^0$.

(c) Similarly, when a small particle is added to a uniform packing of small particles, it occupies a space comparable to that of a neighboring particle. Thus, the ratio of this increase in volume to the solid volume of the added particle v_2 is equal to v_2^0, and the excess free volume $\Delta v_2 = 0$.

(d) If a small particle is added to a uniform packing of large particles, it fills the interstices between large particles, and the increase in volume of the packing is zero, leading to the value of v_2 being equal to 0, and the excess free volume $\Delta v_2 = -v_2^0$.

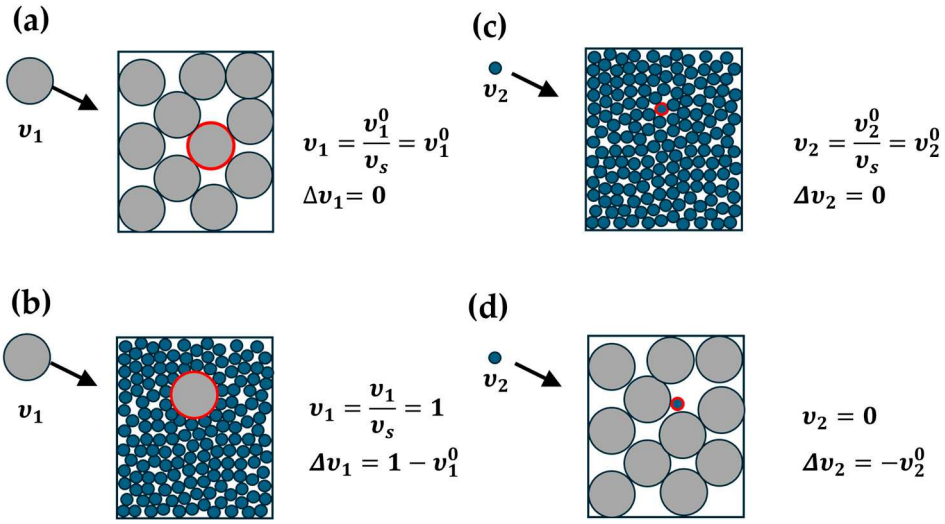

Figure 1. Four scenarios of limiting cases: (**a**) a large particle is added to a uniform packing of large particles, (**b**) a large particle is added to a uniform packing of very small particles, (**c**) a small particle is added to a uniform packing of small particles, and (**d**) a small particle is added to a uniform packing of large particles. The red circle indicates the added particle.

These four scenarios are limiting cases where the particle size ratio $d_2/d_1 \to 0$, providing upper and lower bounds for the values of Δv_i. For general cases, the actual values of Δv_i are within these bounds. Studies on the values of Δv_i for very dense or for very loose sand-silt mixtures have been studied based on experimental measurement [11].

By combining Equations (2) and (3), the total specific volume v can be expressed as

$$v = v_1^0 y_1 + v_2^0 y_2 + \Delta v \tag{5}$$

Here, the total excess free volume Δv in the system is as follows:

$$\Delta v = \Delta v_1 y_1 + \Delta v_2 y_2 \tag{6}$$

As illustrated in Figure 2, line AB represents the total volume before mixing, calculated as $v_1^0 y_1 + v_2^0 y_2$. The curve ACB represents the actual volume after particle mixing. The shaded area between line AB and curve ACB corresponds to the excess free volume Δv.

In the extreme case, where the particle size ratio d_2/d_1 approaches zero, all the voids are filled with small particles, represented by the blue line. Conversely, when all the large particles are embedded in the matrix of small particles, it is represented by the red line. Line AB serves as the upper bound, while the blue line and red line form the lower bound for the system's volume behavior.

In the following sections, we will review various particle packing models and highlight the connection between their assumptions and the concept of excess free volume.

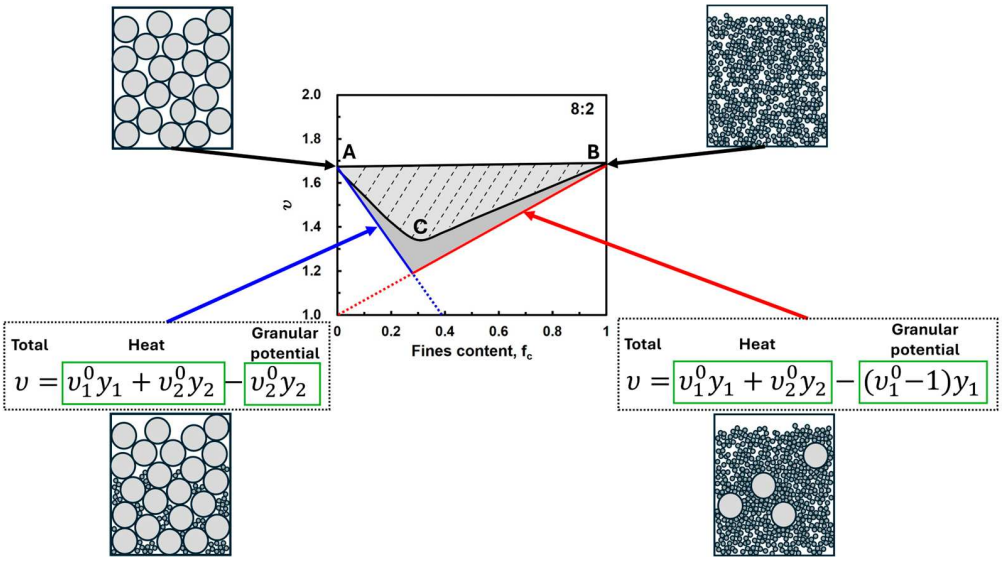

Figure 2. Binary particle packing with varying fines content and its influence on void space. The figure illustrates the relationship between specific volume and fines content. The small plots represent different packing scenarios, demonstrating how granular potential affects the specific volume. The accompanying equation represents the thermodynamics theory applied to the packing model.

3. Review of Models

Three categories of models are briefly reviewed below.

3.1. Limiting Cases

In the 1930s, Westman [12] and Furnas [13] pioneered mathematical models to analyze the packing density of binary particle mixtures. These models account for two distinct packing scenarios:

(1) Dominant by coarse particles: the fine particles are fully accommodated in the voids between the large particles (illustrated by the blue line in Figure 2).

(2) Dominant by fine particles: the large particles are isolated and embedded in the matrix of fine particles (represented by the red line in Figure 2).

The proposed models are expressed as follows:

$$v = v_1^0 y_1 \quad \text{for coarse} - \text{grain dominant region.} \tag{7}$$

$$v = y_1 + v_2^0 y_2 \quad \text{for fine} - \text{grain dominant region.} \tag{8}$$

These equations correspond to the blue and red lines in Figure 2, respectively. These equations can be derived from the concept of excess free volume. In the scenarios of coarse-grain dominance (Figure 1a,d), the excess free volume of the large particles $\Delta v_1 = 0$ (Figure 1a), and for the small particles, $\Delta v_2 = -v_2^0$ (Figure 1d). As a result, the total excess free volume $\Delta v = -v_2^0 y_2$ (see Equation (6)).

On the other hand, when the system is dominant by fine particles (see Figure 1b,c), the excess free volume of fine particles $\Delta v_2 = 0$ (Figure 1c), and for the coarse particles, $\Delta v_1 = 1 - v_1^0$ (Figure 1b), resulting in $\Delta v = \left(1 - v_1^0\right) y_1$ (see Equation (6)).

Substituting these excess volumes into Equation (5), we obtain the following:

$$v = (v_1^0 y_1 + v_2^0 y_2) - v_2^0 y_2 \quad \text{for coarse} - \text{grain dominant region.} \tag{9}$$

$$v = \left(v_1^0 y_1 + v_2^0 y_2\right) - (v_1^0 - 1) y_1 \quad \text{for fine} - \text{grain dominant region.} \tag{10}$$

These two equations match Equations (7) and (8) as proposed by Westman and Hugill [12], and they represent the limiting case models for packings with particle size ratio approaching zero.

3.2. Linear Packing Models

In cases where the particle size ratio does not approach zero, the v vs. f_c curve deviates from the lower bound (as shown in Figure 2). To address this, various models have been developed. A common strategy among these models is to introduce interaction functions that reduce the amount of excess free volume. Two such functions are employed: $f(r)$ for coarse-grain-dominant regions and $g(r)$ for fine-grain dominant regions. The general expressions for these regions are as follows:

$$v = v_1^0 y_1 + v_2^0 y_2 - f(r) v_2^0 y_2 \quad \text{for coarse} - \text{grain dominant region.} \tag{11}$$

$$v = v_1^0 y_1 + v_2^0 y_2 - g(r)(v_1^0 - 1) y_1 \quad \text{for fine} - \text{grain dominant region.} \tag{12}$$

As $f(r) = g(r) = 0$, the equations represent the upper bound, and as $f(r) = g(r) = 1$, they represent the lower bound. In general, the interaction functions depend on the size ratio r, with $0 < f(r) < 1$ and $0 < g(r) < 1$, producing a curve that can be approximated by two linear segments.

Ben Aim and Goff [14] proposed a model that assumes that the coarse-grain-dominant region follows the lower bound ($f(r) = 1$) but introduced $g(r)$, referred to as the "wall effect", which accounts for the influence of coarse particles embedded in a fine-particle matrix [15].

$$g(r) = 1 - \frac{5}{16}\left((1+2r)^{\frac{3}{2}} - 1\right)/(v_1^0 - 1) \tag{13}$$

When $r = 0$, it represents the lower bound.

In 1986, Stovall et al. [16] proposed the "linear packing density model" of particle mixtures. In this model, $f(r)$ is defined based on a critical cavity size ($r_0 = 0.2$). For fine particles smaller than r_0 (i.e., $r \leq 0.2$), $f(r) = 1$, corresponding to the limiting case. For fine particles larger than r_0 (i.e., $r > 0.2$), $f(r)$ accounts for the loosening effect on the coarse-grain network:

$$f(r) = 1 - \frac{1 - (r_0/r)^3}{\left(\frac{(v_1^0 - 1)(1 - r_0^3)}{v_1^0} - 3r_0^3\right)(1 - r) + \left(1 - r_0^3\right)} \quad r > r_0 \tag{14}$$

$$g(r) = 1 - r \tag{15}$$

When $r \to 0$, $g(r) = 1$, leading to the lower bound. As $r = 1$ ($d_2 = d_1$), $f(r) = g(r) = 0$, representing the upper bound.

In 1996, Yu, Zou, and Standish [17] introduced different expressions for the interaction functions $f(r)$ and $g(r)$:

$$f(r) = (1 - r)^{3.3} + 2.8r(1 - r)^{2.7} \tag{16}$$

$$g(r) = (1 - r)^{2.0} + 0.4r(1 - r)^{3.7} \tag{17}$$

These functions $f(r)$ and $g(r)$ are specific to spherical particles. Yu, Zou, and Standish [17] have further modified these functions for non-spherical particles, though only a limited range of shapes were considered.

De Larrard's "Compressible Packing Model" [18] built upon Stovall's work, incorporating a compaction index K. The model accounts for the packing process via a compaction index K. For a virtual packing, when $K \to \infty$, the model is similar to Equations (11) and (12), with interaction functions given by the following:

$$f(r) = \sqrt{1 - (1 - r)^{1.02}} \tag{18}$$

$$g(r) = (1-r)^{1.5} \tag{19}$$

Chang, Wang, and Ge [19] have proposed a model for sand-silt mixtures, introducing filling and embedding coefficients for soil particles, which have a large variation in shape. The functions are as follows:

$$f(r) = (1-r)^{p} \tag{20}$$

$$g(r) = (1-r)^{s} \tag{21}$$

The exponents p and s are correlated to particle shapes, which can be calibrated from experimental results.

Kim and Seo [20] evaluated the performance of the Chang et al. [19] model by comparing the measured and predicted void ratios for the three sand–sand mixture samples at various fines contents. They found that although the use of two parameters, p and s, in Equations (20) and (21) provides more accurate predictions of the measured results, the model still produces reasonable predictions even when assuming $p = s$. This suggests that with the one-parameter model, only a single interaction function is necessary (i.e., $\lambda(r) = f(r) = g(r)$).

Table 1 provides a comprehensive overview of various linear packing models developed by different researchers, specifically focusing on the interaction functions $f(r)$ and $g(r)$. These functions are crucial for understanding how particles of different sizes interact in a mixture, influencing the packing density and volume change. The function $f(r)$ typically represents the interaction in the coarse-grain dominant region, while $g(r)$ characterizes the interactions in the fine-grain dominant region. Both functions are dependent on the particle size ratio, r.

Table 1. Summary of interaction functions $f(r)$ and $g(r)$ in linear packing models.

Researcher(s)	*f*(*r*) Expression	*g*(*r*) Expression
Aim and Goff [14]	$f(r) = 1$ (Lower bound)	$g(r) = 1 - \frac{5}{16}\left(1 + 2r^{3/2}\right)^{-1}$
Stovall et al. [16]	$f(r) = 1 - \frac{1-(r_0/r)^3}{\left(\frac{(v_1^0-1)(1-r_0^3)}{v_1^0} - 3r_0^3\right)(1-r)+\left(1-r_0^3\right)}$ for $r > r_0$	$g(r) = 1 - r$
Yu et al. [17]	$f(r) = (1-r)^{3.3} + 2.8r(1-r)^{2.7}$	$g(r) = (1-r)^{2.0} + 0.4r(1-r)^{3.7}$
De Larrard [18]	$f(r) = \sqrt{1-(1-r)^{1.02}}$	$g(r) = (1-r)^{1.5}$
Chang, Wang, and Ge [19]	$f(r) = (1-r)^{p}$	$g(r) = (1-r)^{s}$

These interaction functions are key to accounting for effects such as the "wall effect", where coarse particles influence the packing of fine particles, and the "loosening effect", where fine particles loosen the structure of a coarse-particle matrix. Different models use these functions to address complex particle interactions in various mixtures.

By summarizing these models, Table 1 provides a useful comparison of how different researchers approach the prediction of volume changes due to particle mixing in coarse- and fine-grain regions, taking into account the size ratio and associated physical phenomena.

The linear packing models for predicting the packing behavior of binary mixtures typically rely on two straight lines, one representing the coarse-grain dominant region and the other for the fine-grain dominant region. However, when the particle size ratio $r > 0.22$, these models often fail to accurately predict experimental results due to the non-linearity of the v vs. y_2 curve. This non-linearity becomes especially pronounced in transitional regions where neither coarse nor fine particles dominate entirely.

3.3. Non-Linear Packing Models

There are two primary approaches used to achieve the desired non-linear curve in packing models: (1) compressible packing models and (2) models with non-linear functions.

3.3.1. Compressible Packing Models

This approach is based on the assumption that particles are deformable. The compressible packing model (CPM), introduced by de Larrard [18], includes a compaction index K, which allows the prediction of a non-linear curve shape.

The compaction index K relates virtual volume and real volume by the following:

$$v_{virtual} = v\frac{K}{1+K} \tag{22}$$

When $K \to \infty$, the packing is considered virtual (non-deformable particles), with the packing density predicted using linear models for coarse-grain and fine-grain dominant regions.

For smaller values of K, the compaction effect introduces a smooth non-linear behavior. The value of K varies based on the sample preparation method and can differ for samples prepared by pouring, tamping with a rod, vibration, or compression.

Roquier [21,22] enhanced the compressible packing model by proposing new formulations for the interaction functions (wall effect and loosening effect coefficients) and new values of K. The improvements account for size ratio r, the real specific volumes of each species, and the compaction index K.

3.3.2. Models with Non-Linear Functions

The second approach involves treating the excess free volume Δv as a non-linear function of the higher order of solid fractions y_1 and y_2 for each species:

$$\Delta v = \Delta v(r, y_1, y_2) \tag{23}$$

From Equation (5), a higher order function of Δv results in a non-linear curve of specific volume v vs. y_2. There are two approaches to model Δv: (1) treat Δv as a single function covering the entire range of fines content and (2) use two distinct functions—one for the coarse-grain dominant region and the other for the fine-grain dominant region.

1. Models with a single non-linear function

Instead of applying separate non-linear functions to each dominant region, one approach is to use a single non-linear function across the entire range of fines content. This simplifies the mathematical structure and allows the specific volume of the packing mixture to be expressed as follows:

$$v = v_1^0 y_1 + v_2^0 y_2 - \Delta v(r, y_1, y_2) \tag{24}$$

In 1976, Toufar et al. [23] proposed the following non-linear function:

$$\Delta v(r, y_1, y_2) = y_1\left(v_1^0 - 1\right)k_d k_s \tag{25}$$

This function incorporates two factors: k_d, which depends on size ratio, and k_s, a statistical factor that is a linear function of volume fractions y_1 and y_2. This results in Δv being a higher order function of volume fractions. Goltermann et al. [24] made a minor correction to the value of k_s in 1997.

Han et al. [25] considered another expression for the non-linear function,

$$\Delta v(r, y_1, y_2) = y_1\left(v_1^0 - 1\right)B \tag{26}$$

Here, B is based on geometric considerations of the probability for one coarse particle to come into contact with a fine particle. The expression of B is a function of r, y_1, and y_2. When the two species have the same diameter (i.e., r = 1), B = 0, representing the upper bound, while B = 1 reduces the equation to the lower bound solution for the fine-grain dominant region.

Wu and Li [26] extended Han et al.'s work to analyze sediment mixtures. They introduced several ranges of B values for various conditions such as pebble-sand mixtures, sand-clay mixtures, under hydrostatic pressures, and in river environments.

2. Models with two dominant packing structures

Kwan et al. [27] proposed two non-linear functions separately for coarse-grain and fine-grain dominant regions. Besides the loosening effect coefficient $a(r)$ (equivalent to $f(r)$) and the wall effect coefficient $b(r)$ (equivalent to $g(r)$), they introduced the wedging effect coefficient $c(r)$, which affects both coarse-grain and fine-grain dominant regions. The wedge effect involves non-linear exponential forms of solid fractions.

$$\Delta v(r, y_1, y_2) = (1 - a(r))v_2^0 y_2 - c(r)a(r)v_2^0 y_2(3.8^{y_2} - 1) \quad \text{for coarse} - \text{grain dominant region.} \tag{27}$$

$$\Delta v(r, y_1, y_2) = (1 - b(r))(v_1^0 - 1)y_1(1 - c(r)(2.6^{y_1} - 1)) \quad \text{for fine} - \text{grain dominant region.} \tag{28}$$

The expressions of $a(r)$, $b(r)$, and $c(r)$ are complex, accounting for various particle shapes under compacted or uncompacted conditions.

Yu and Standish [28] developed a non-linear packing model, named the "linear—mixture packing model", which combines their linear packing model [17] with a cubic non-linear "mixture model". This model presents the non-linear function Δv as two separate functions of the size ratio r (where $r = d_2/d_1$):

$$\Delta v(r, y_1, y_2) = \beta_{12} y_1 y_2 + \gamma_{12} y_1 y_2 (y_1 - y_2) \tag{29}$$

Here, β_{12} and γ_{12} are, respectively, the quadratic and the cubic coefficients [29]. β_{12} and γ_{12} can be determined through a fitting procedure described by Yu and Standish [28] and are found to be dependent on size ratio and initial specific volume v_i^0.

The model considers three conditions.

For $r \geq 0.741$ (near uniform packing), $\beta_{12} = \gamma_{12} = 0$, representing the upper bound.

For $0.741 > r > 0.154$, non-linear behavior exhibits, with values of β_{12} and γ_{12} determined by the fitting method suggested in [29]. The binary mixture of particles is mainly characterized by occupation (mixing effect).

For $r < 0.154$, where the small particle size is less than the cavity size, it simplifies to the linear packing model [17], characterized by filling (unmixing effects).

At $r = 0.154$, a slight discontinuity in the estimated packing densities occurs when transitioning between the linear and non-linear models.

Liu et al. [30] developed a model proposing two non-linear functions for two dominant regions. Both are expressed as quadratic functions with respect to solid fractions y_1 and y_2.

It is noted that all of the non-linear functions $\Delta v(r, y_1, y_2)$ discussed here are phenomenological constructs. Using a single function of Δv for the entire range of fines content would result in a highly complex function. Since the packing structure can be broadly divided into two dominant regions, it is more reasonable to establish two non-linear functions—one for coarse-grain and one for fine-grain dominant regions—rather than a single function that covers the entire region.

Moreover, the packing structure cannot always be simplified into these two dominant types, particularly when dealing with larger size ratios. In reality, the packing structure is a dual skeleton composed of both species, and it continuously transitions from one dominant type to another as the fines content changes [31].

To further consider the influence of packing structure, Chang and Deng [32] introduced a model that considers the variation of the packing skeleton with fines content. They hypothesized a characteristic size λ ($d_1 > \lambda > d_2$), which varies continuously with packing composition, $\lambda(d_1, d_2, y_1, y_2)$. In this context, the size ratio $\frac{\lambda}{d_1}$ is used to characterize the excess free volume of the large particle species, representing the filling mechanism. The

size ratio $\frac{d_2}{\lambda}$ is used to characterize the excess free volume of the small particle species, representing the embedment mechanism. This model effectively accounts for both filling and embedment mechanisms in particle packings. The total excess free volume of the packing is expressed as a function of these ratios, given by

$$\Delta v = \left(1 - \frac{\lambda}{d_1}\right)^{\eta} (v_1^0 - 1) + \left(1 - \frac{d_2}{\lambda}\right)^{\eta} v_2^0 \tag{30}$$

The characteristic length $\lambda(d_1, d_2, y_1, y_2)$ is determined by the minimization of excess free volume.

$$\frac{d(\Delta v)}{d\lambda} = 0 \tag{31}$$

This model was later contextualized within the Edward thermodynamics theory [8], where the excess free volume in Equation (30) is analogous to chemical potential. In [11], Equation (31) was derived from the second law of thermodynamics, which stipulates that the Gibbs volume potential must be minimized for a closed system to be at equilibrium at a constant compactivity [8].

Table 2 provides a summary of the strengths and limitations of the different particle packing models discussed in this section, categorized into three main types: limiting case models, linear packing models, and non-linear packing models.

Table 2. Summary table: Strengths and limitations of models.

Model Type	Strength/Limitation	Guideline on Size Ratio
Limiting Case Models	Simple and intuitive/Valid only for limiting case	Size ratio smaller than 0.1 or larger then 0.8
Linear Packing Models	Accounts for interaction between particles/ In accurate in transition zone	Size ratio smaller than 0.2
Non-Linear Packing Models	Captures more complex particle interactions/ Requires more parameters	Size ratio smaller than 0.8 or larger than 0.2

Building on their foundational formulations, several bi-dispersed models have been extended to predict the packing density of multi-component particle mixtures. These include Mooney [33], Stovall [16], Yu [17,29], De Larrard [18], Roquier [21,22], Chang [32], and Liu [30]. These multi-sized models are not included in this review.

4. Geotechnical Application

Although particle packing models are primarily limited to predicting the packing density of soil mixtures, they are highly valuable in geotechnical engineering due to the strong correlation between soil density and its properties, as well as the performance of granular materials. In the context of geotechnical engineering, we examine the application of particle packing models in three important areas: (1) estimating the maximum, minimum, and critical state void ratios for sand-silt mixtures, (2) connecting the packing model to the inter-granular void ratio, and (3) predicting the mechanical properties of binary mixtures based on relative density.

4.1. Estimating Maximum, Minimum, and Critical State Void Ratios

The variation in maximum void ratio with respect to fines content in sand-silt mixtures is driven by the same mechanisms that influence the variation of minimum void ratio [34]. As a result, particle packing models can reliably estimate both minimum and maximum void ratios for sand-silt mixtures as fines content changes. This has been validated across various sand-silt mixtures with different fines contents [34]. Figure 3, for example, shows the comparison of predicted and measured results of maximum and minimum void ratios

predicted using the method by Chang and Deng [32]. The input material parameter η is 2.1 for silica mixture and 3.9 for Hokksund mixture.

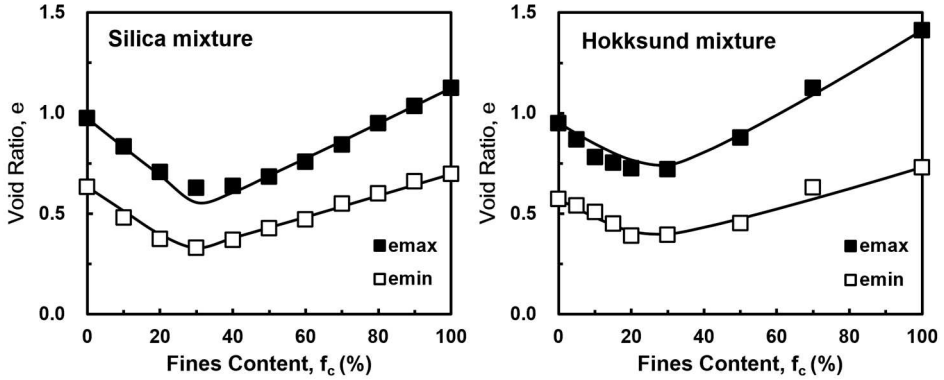

Figure 3. Comparison of predicted and measured maximum and minimum void ratios of silica and Hokksund mixtures.

It is important to note that in situ soil density, by itself, is not correlated well with mechanical properties. Instead, relative density serves as a better indicator. Therefore, reliable estimation of both minimum and maximum void ratios is essential for understanding soil behavior.

Furthermore, the variation in critical state void ratio with fines content is governed by the same mechanisms that influence the variation of minimum void ratio. This allows particle packing models to estimate critical state void ratios for sand-silt mixtures as fines content changes. In Figure 4a, the symbols represent the experimentally measured critical state void ratios versus effective stress for various fines contents in the Foundry mixture. In Figure 4b, the critical state void ratios measured at effective stresses of 40, 400, and 1400 MPa are plotted against fines content. The solid lines represent the predicted results using the model by Chang and Deng [32] with parameter η = 3.2. The comparison illustrates the model's ability to predict critical state void ratios.

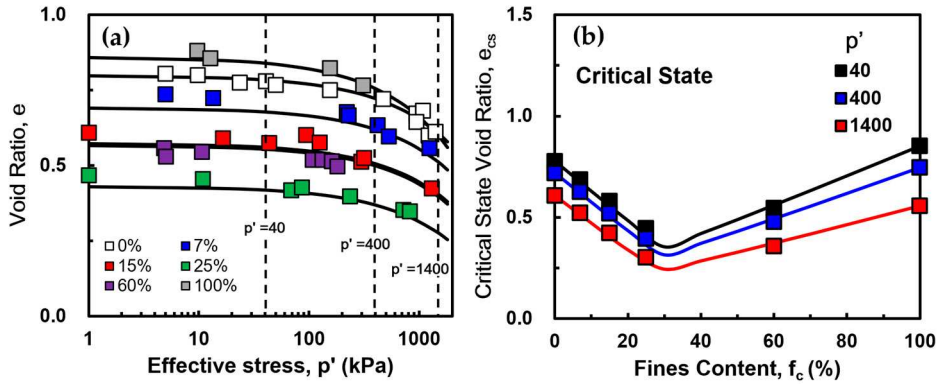

Figure 4. (**a**) Experimentally measured critical state void ratios versus effective stress for packings with various fines content. (**b**) The comparison of predicted and measured critical state void ratios with fines content for three different effective stresses. The void ratios at three effective stress levels, represented by dotted lines in Figure 4a, are plotted in Figure 4b for different fines contents.

By predicting minimum, maximum, and critical state void ratios, particle packing models provide a more comprehensive metric for estimating the mechanical performance of sand-silt mixtures. This is crucial for designing foundations, embankments, and other geotechnical structures.

4.2. Connection to Inter-Granular Void Ratio

The concept of inter-grain void ratio [35,36] has been widely used to characterize the mechanical behavior of sand-silt mixtures, such as peak stress ratio, yield strength ratio [37], shear modulus (wave velocity) [38], static and cyclic strength, and the liquefaction potential [36,39–41]. In this regard, a transitional fines content (f_{tr}) is defined to indicate whether the mixture behaves predominantly as coarse-grained or as fine-grained.

At low fines content ($f_c < f_{tr}$), the fine particles do not carry load and thus are assumed to not contribute to the mechanical properties, and the mixture behaves as a coarse-grain network. Oppositely, when the fines content is high ($f_c > f_{tr}$), coarse grains, embedded in the network of fine grains, play a limited role in the mechanical behavior. Thus, the mixture behaves as a fine-grain network. The behavior of a sand-silt mixture depends more on whether the fines content is above or below the f_{tr} rather than on the actual fines content itself. The value of f_{tr} can be determined from index data or from the results of triaxial tests.

In case of low fines content, some fine particles may still carry load. To account for these active fine particles, Thevanayagam et al. [36] introduced an "equivalent" inter-granular void ratio e_c^* by

$$e_c^* = \frac{e + (1-b)f_c}{1-(1-b)f_c} \qquad f_c < f_{tr} \tag{32}$$

The variable e_c^* is a function of the void ratio e and the fines content f_c of silty sand. The parameter b was defined as the active fraction of fines in the mixture, varying between 0 and 1. However, it is not clear how to determine the exact amount of active fraction of fines in a soil mixture. Thus, the value of b cannot be measured directly. Thevanayagam et al. [36] provided back-calculated values from experimental results. Some researchers suggest empirical expressions as a function of fines content.

The particle packing framework can be used to estimate e_c^* [42]. This is made possible by a conjecture that e_c^* for a sand-silt mixture at a given fines content f_c is equal to the void ratio of pure sand under the same relative density of the sand-silt mixture. In linear particle packing models, the value of b corresponds to the slope of the plot of e versus f_c. An explicit expression of b can be derived as a function of specific volumes of pure sand v_1^0 and pure silt v_2^0, along with the particle size ratio:

$$b = \frac{v_2^0}{v_1^0}\left(1 - \left(1 - \frac{d_{50}}{D_{50}}\right)^p\right) \tag{33}$$

where v_i^0 represents the specific volume of each species. The two specific volumes v_1^0 and v_2^0, in general, are different due to the difference in their particle sizes and shapes. In the condition that $v_1^0 = v_2^0$, the equation simplifies to

$$b = 1 - \left(1 - \frac{d_{50}}{D_{50}}\right)^p \tag{34}$$

This formula of parameter b has been validated through comparisons between predicted and measured results for various sand-silt mixtures [42], showing significant influence when the specific volumes of the two species differ substantially.

4.3. Predicting Mechanical Properties and Relative Density

Particle packing models can also predict mechanical properties based on relative density, such as stress ratio, yield strength ratio, and shear modulus, for different fines contents.

4.3.1. Stress Ratio and Yield Strength Ratio

The experimental results by Yang et al. [37] were selected in this study. Shear strength was measured from undrained triaxial compression tests (CIU) conducted on sand-silt mixtures with varying fines content ranging from 0% to 94%. The mixtures were prepared

using Hokksund sand and Chengbei silt. The sand is composed primarily of quartz, feldspar, and mica, characterized by sharp, cubical particles with a mean particle size $D_{50} = 0.44$ mm. The non-plastic silt, with a $d_{50} = 0.032$ mm, was used for the fines, and mixtures were created to achieve different fines content.

Isotropically consolidated undrained triaxial compression tests were conducted on sand-silt mixtures under confining pressures ranging from 50 to 150 kPa. The initial relative density of the samples, which varies in fines content, ranges from 0.2 to 0.8. Due to the effects of consolidation from the applied confining pressures, the relative density of the samples increased slightly.

The undrained strength (expressed as stress ratio) for all samples is plotted in Figure 5a. The yield strength ratio for all samples is illustrated in Figure 5b.

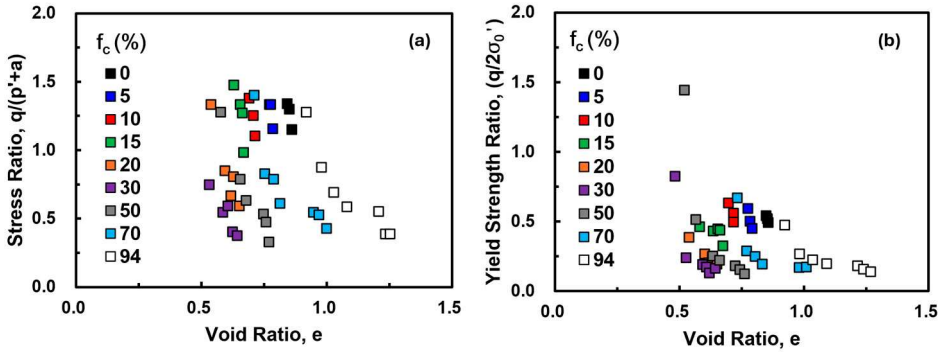

Figure 5. Consolidated undrained triaxial compression experimental results for sand-silt mixtures with various fines content (f_c from 0% to 94%): (**a**) stress ratio versus void ratio, (**b**) yield strength ratio versus void ratio.

Figure 6 illustrates the maximum and minimum void ratios determined in accordance with ASTM standards (represented by symbols) compared with the predicted maximum and minimum void ratios (depicted by solid lines) for various fines content. The solid lines were predicted using the non-linear model by Chang and Deng [32]. The input data are provided in Table 3. The predicted and measured results are in good agreement. The dashed lines represent relative densities ranging from 0.1 to 0.9. Additionally, the test results of each sample's undrained stress ratio and yield strength ratio are plotted in symbols.

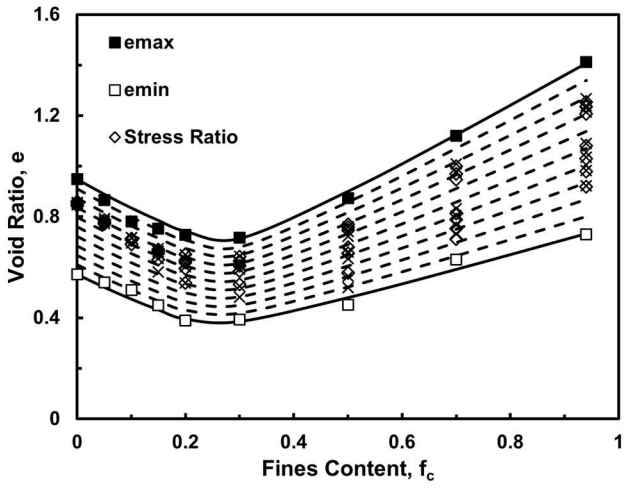

Figure 6. Minimum and maximum void ratios for sand-silt mixtures with varying fines content. Symbols represent the void ratio of the samples after consolidation. The samples were used in triaxial tests to measure the stress ratio and yield strength ratio. The dashed line indicates the relative densities of the sand-silt mixtures as the fines content varies.

Table 3. The model's parameters for the sand-silt mixtures.

Soil Type	Size (mm)	e_{max}	e_{min}	η
Sand	0.44	0.949	0.572	4.0
Silt	0.032	1.480	0.770	4.0

Using the predicted values of maximum and minimum void ratios, the relative density for each sample at failure was calculated, and the relationships between relative density, stress ratio, and yield strength were then plotted in Figure 6.

It is noted that in Figure 5, the stress ratio and yield strength ratio do not show clear correlations with the void ratio. However, when the measured results are plotted along relative density in Figure 7, three distinct types of behavior emerge:

1. For f_c < 15%, the behavior is coarse-grain dominant, similar to pure sand.
2. For f_c > 50%, the behavior is fine-grain dominant, similar to pure silt.
3. For 15% < f_c < 50%, the behavior is a mix of the two, showing transitional characteristics.

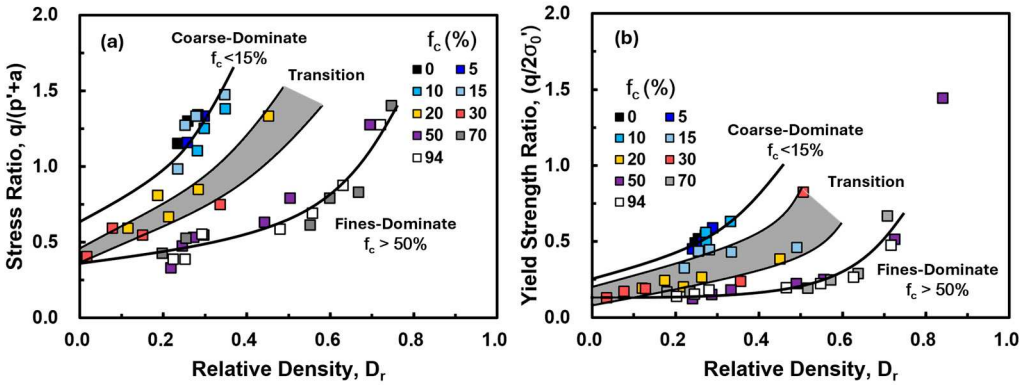

Figure 7. (**a**) Relationship between stress ratio and relative density and (**b**) relationship between yield strength ratio and relative density of sand-silt mixtures with varying fines content. For f_c < 15% (coarse-grain dominant) or f_c > 50% (fine-grain dominant), the relationship can be represented by solid lines. For f_c in between 15% and 50% (transition zone), the relationship is scattered in a zone.

This range of fines content significantly affects the relationship between mechanical properties. The first two behaviors align with the concept of inter-grain void ratio. In Figure 6, the transitional fines content (f_{tr}) is approximately 26%. Mixtures with f_c < 26% exhibit coarse-grain dominant behavior, while those with f_c > 26% show fine-grain dominant behavior. The third type of behavior in Figure 7 provides a more refined description of the mixture behavior around this transitional fines content f_{tr}.

The particle packing model is a useful tool that provides a better assessment of relative density, which is a critical factor in evaluating the risk of soil liquefaction and serves as guidance for construction and quality control.

4.3.2. Shear Modulus

In this study, particle packing models are applied to interpret the acoustic properties of sandstone. Data from Han et al. [43] were used, with samples taken from well cores and quarries. These samples ranged in dimensions from 2.0 to 5.0 cm in length and 5.0 cm in diameter, ensuring the sample dimensions were at least 100 times the average grain size. The shear wave velocities (V_s) were measured using pulse transmission techniques, under confining pressures of 40 MPa and pore pressures of 1.0 MPa, to simulate deep subsurface conditions. The shear modulus (G) was then calculated using the formula $G = \rho V_s^2$, where ρ is the density of the sandstone.

Figure 8 presents results from tests conducted on 75 sandstone samples with clay content from 0% to 50%. The maximum and minimum void ratios were predicted using

the non-linear model by Chang and Deng [32] and are represented by the solid lines shown in Figure 9a. The dashed lines represent the lines of relative density ranging from 0.1 to 0.9. The input data for these predictions are provided in Table 4.

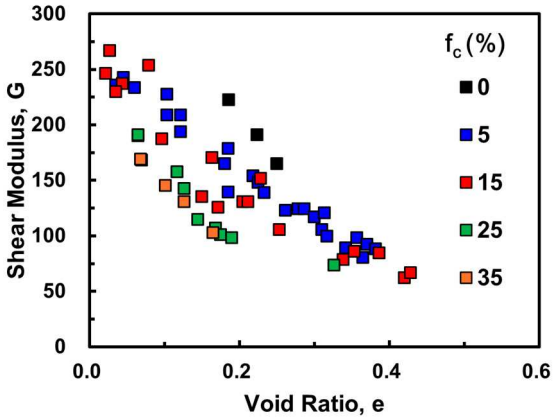

Figure 8. Shear modulus test results for 75 sandstone samples with varying void ratios and clay content.

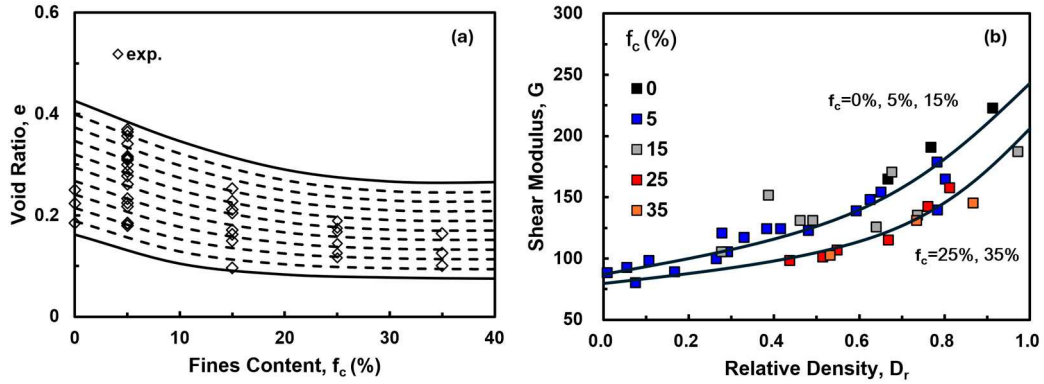

Figure 9. (**a**) Maximum and minimum void ratios versus fines content and (**b**) shear modulus versus relative density for sandstone mixtures.

Table 4. The model's parameters for the sandstone sample.

Soil Type	Size (mm)	e_{max}	e_{min}	η
Sandstone	0.2	0.426	0.162	4.0
Silty size clay	0.015	0.480	0.100	4.0

The measured modulus for each sample is plotted in symbols in Figure 9a. Using the predicted values of maximum and minimum void ratios, the relative density for each sample was calculated. The relationships between relative density and shear modulus were plotted in Figure 9b, which reveals two distinct types of behavior: samples with $f_c = 0\%, 5\%, 15\%$ and samples with $f_c = 25\%, 35\%$. These two groups exhibit different trends in the relationship between relative density and shear modulus.

In summary, relative density (compared to void ratio alone) offers a more detailed and useful metric for understanding and predicting mechanical behavior in engineering applications.

5. Conclusions

Various particle packing models can be classified into three categories: limiting case models, linear packing models, and non-linear packing models. Each model has distinct mathematical formulations. Despite these differences, our review indicated that the underlying physics across all models is rooted in the concept of "excess free volume", which

is crucial for understanding the assumptions behind the models and predicting volume change behavior in sand-silt mixtures.

Current particle packing models are primarily focused on predicting packing density. However, beyond this, there is potential to analyze the statistical properties of free volume associated with the void distribution in soil mixtures using analytical methods from the framework of Edwards thermodynamics. This approach can offer valuable insights into soil microstructures, shedding light on the granular arrangements and interactions at the microscopic level. This area remains insufficiently explored and warrants further research to better understand the complex behavior of soil mixtures.

Particle packing models have been applied in fields such as high-performance concrete, ceramics, sediments, and the pharmaceutical industry. In geotechnical engineering, we examine its use in three key areas: (1) estimating maximum, minimum, and critical state void ratios for binary mixtures, (2) connecting the packing model to the inter-granular void ratio, and (3) predicting the mechanical properties of binary mixtures based on relative density. Our findings indicate that particle packing models are a valuable tool for improving the assessment of minimum, maximum, and critical state void ratios and shear modulus, which are essential for developing constitutive models and characterizing the mechanical properties of sand-silt mixtures.

Author Contributions: Conceptualization, C.S.C.; Methodology, C.S.C.; Software, C.S.C. and J.C.; Validation, J.C.; Investigation, C.S.C.; Data curation, J.C.; Writing—original draft, C.S.C.; Writing—review & editing, J.C.; Visualization, J.C.; Supervision, C.S.C.; Funding acquisition, C.S.C. All authors have read and agreed to the published version of the manuscript.

Funding: This research was funded by the National Science Foundation under the research grant CMMI-1917238.

Data Availability Statement: Publicly available datasets were analyzed in this study. These data can be found here: [https://doi.org/10.1016/j.soildyn.2004.11.027, https://doi.org/10.1190/1.1442062], accesses on 1 August 2024.

Acknowledgments: This work was supported by the National Science Foundation under the research grant CMMI-1917238.

Conflicts of Interest: The authors declare no conflicts of interest.

References

1. de Larrard, F.; Sedran, T. Optimization of Ultra-High-Performance Concrete by the Use of a Packing Model. *Cem. Concr. Res.* **1994**, *24*, 997–1009. [CrossRef]
2. Wang, Z.M.; Kwan, A.K.H.; Chan, H.C. Mesoscopic Study of Concrete I: Generation of Random Aggregate Structure and ®nite Element Mesh. *Comput. Struct.* **1999**, *70*, 533–544. [CrossRef]
3. Du, W.; Singh, M.; Singh, D. Binder Jetting Additive Manufacturing of Silicon Carbide Ceramics: Development of Bimodal Powder Feedstocks by Modeling and Experimental Methods. *Ceram. Int.* **2020**, *46*, 19701–19707. [CrossRef]
4. Liu, D.-M. Particle Packing and Rheological Property of Highly-Concentrated Ceramic Suspensions: Φm Determination and Viscosity Prediction. *J. Mater. Sci.* **2000**, *35*, 5503–5507. [CrossRef]
5. Muzzio, F.J.; Shinbrot, T.; Glasser, B.J. Powder Technology in the Pharmaceutical Industry: The Need to Catch up Fast. *Powder Technol.* **2002**, *124*, 1–7. [CrossRef]
6. Holtz, R.D.; Kovacs, W.D.; Sheahan, T.C. *An Introduction to Geotechnical Engineering*, 2nd ed.; Pearson: London, UK, 2011; ISBN 978-9332507617.
7. Lade, P.; Liggio, C.; Yamamuro, J. Effects of Non-Plastic Fines on Minimum and Maximum Void Ratios of Sand. *Geotech. Test. J.* **1998**, *21*, 336–347. [CrossRef]
8. Chang, C.S. Jamming Density and Volume-Potential of a Bi-Dispersed Granular System. *Geophys. Res. Lett.* **2022**, *49*, e2022GL098678. [CrossRef]
9. Silbey, R.J.; Alberty, R.A.; Bawendi, M.G. *Physical Chemistry*, 4th ed.; Wiley: Hoboken, NJ, USA, 2004.
10. Chang, C.S.; Deng, Y. Packing Potential Index for Binary Mixtures of Granular Soil. *Powder Technol.* **2020**, *372*, 148–160. [CrossRef]
11. Chang, C.S.; Deng, Y. Compaction of Bi-Dispersed Granular Packing: Analogy with Chemical Thermodynamics. *Granul. Matter* **2022**, *24*, 58. [CrossRef]
12. Westman, A.E.R.; Hugill, H.R. The Packing of Particles. *J. Am. Ceram. Soc.* **1930**, *13*, 767–779. [CrossRef]

13. Furnas, C.C. Grading Aggregates—I.—Mathematical Relations for Beds of Broken Solids of Maximum Density. *Ind. Eng. Chem.* **1931**, *23*, 1052–1058. [CrossRef]
14. Aïm, R.B.; Goff, P.L. Effet de Paroi Dans Les Empilements Désordonnés de Sphères et Application à La Porosité de Mélanges Binaires. *Powder Technol.* **1968**, *1*, 281–290. [CrossRef]
15. Roquier, G. A Century of Granular Packing Models. *Powder Technol.* **2024**, *441*, 119761. [CrossRef]
16. Stovall, T.; de Larrard, F.; Buil, M. Linear Packing Density Model of Grain Mixtures. *Powder Technol.* **1986**, *48*, 1–12. [CrossRef]
17. Yu, A.B.; Zou, R.P.; Standish, N. Modifying the Linear Packing Model for Predicting the Porosity of Nonspherical Particle Mixtures. *Ind. Eng. Chem. Res.* **1996**, *35*, 3730–3741. [CrossRef]
18. Larrard, F.D. *Concrete Mixture Proportioning: A Scientific Approach*; CRC Press: London, UK, 1999; ISBN 978-0-429-17909-9.
19. Chang, C.S.; Wang, J.-Y.; Ge, L. Modeling of Minimum Void Ratio for Sand–Silt Mixtures. *Eng. Geol.* **2015**, *196*, 293–304. [CrossRef]
20. Kim, M.; Seo, H. Evaluation of One- and Two-Parameter Models for Estimation of Void Ratio of Binary Sand Mixtures Deposited by Dry Pluviation. *Granul. Matter* **2019**, *21*, 71. [CrossRef]
21. Roquier, G. The 4-Parameter Compressible Packing Model (CPM) Including a New Theory about Wall Effect and Loosening Effect for Spheres. *Powder Technol.* **2016**, *302*, 247–253. [CrossRef]
22. Roquier, G. Evaluation of Three Packing Density Models on Reference Particle-Size Distributions. *Granul. Matter* **2024**, *26*, 7. [CrossRef]
23. Toufar, W.; Born, M.; Klose, E. *Contribution of Optimisation of Components of Different Density in Polydispersed Particles Systems*; Freiberger: Saxony, Germany, 1976.
24. Goltermann, P.; Johansen, V.; Palbøl, L. Packing of Aggregates: An Alternative Tool to Determine the Optimal Aggregate Mix. *Mater. J.* **1997**, *94*, 435–443. [CrossRef]
25. Han, Q.W.; Wang, Y.C.; Xing, X.L. Initial Specific Weight of Deposits. *J. Sediment. Res.* **1981**, *1*, 1–13.
26. Wu, W.; Li, W. Porosity of Bimodal Sediment Mixture with Particle Filling. *Int. J. Sediment Res.* **2017**, *32*, 253–259. [CrossRef]
27. Kwan, A.K.H.; Chan, K.W.; Wong, V. A 3-Parameter Particle Packing Model Incorporating the Wedging Effect. *Powder Technol.* **2013**, *237*, 172–179. [CrossRef]
28. Yu, A.B.; Standish, N. An Analytical—Parametric Theory of the Random Packing of Particles. *Powder Technol.* **1988**, *55*, 171–186. [CrossRef]
29. Yu, A.B.; Standish, N. Estimation of the Porosity of Particle Mixtures by a Linear-Mixture Packing Model. *Ind. Eng. Chem. Res.* **1991**, *30*, 1372–1385. [CrossRef]
30. Liu, Z.-R.; Ye, W.-M.; Zhang, Z.; Wang, Q.; Chen, Y.-G.; Cui, Y.-J. A Nonlinear Particle Packing Model for Multi-Sized Granular Soils. *Constr. Build. Mater.* **2019**, *221*, 274–282. [CrossRef]
31. Chang, C.S.; Deng, Y. A Particle Packing Model for Sand–Silt Mixtures with the Effect of Dual-Skeleton. *Granul. Matter* **2017**, *19*, 80. [CrossRef]
32. Chang, C.S.; Deng, Y. A Nonlinear Packing Model for Multi-Sized Particle Mixtures. *Powder Technol.* **2018**, *336*, 449–464. [CrossRef]
33. Mooney, M. The Viscosity of a Concentrated Suspension of Spherical Particles. *J. Colloid Sci.* **1951**, *6*, 162–170. [CrossRef]
34. Chang, C.S.; Wang, J.Y.; Ge, L. Maximum and Minimum Void Ratios for Sand-Silt Mixtures. *Eng. Geol.* **2016**, *211*, 7–18. [CrossRef]
35. Thevanayagam, S.; Mohan, S. Intergranular State Variables and Stress–Strain Behaviour of Silty Sands. *Géotechnique* **2000**, *50*, 1–23. [CrossRef]
36. Thevanayagam, S.; Martin, G.R. Liquefaction in Silty Soils—Screening and Remediation Issues. *Soil Dyn. Earthq. Eng.* **2002**, *22*, 1035–1042. [CrossRef]
37. Yang, S.L.; Sandven, R.; Grande, L. Instability of Sand–Silt Mixtures. *Soil Dyn. Earthq. Eng.* **2006**, *26*, 183–190. [CrossRef]
38. Yang, S.; Lacasse, S.; Forsberg, C.F. Application of Packing Models on Geophysical Property of Sediments. In Proceedings of the 16th International Conference on Soil Mechanics and Geotechnical Engineering, Osaka, Japan, 12–16 September 2005.
39. Xenaki, V.C.; Athanasopoulos, G.A. Discussion of "Effects of Nonplastic Fines on the Liquefaction Resistance of Sands" by Carmine P. Polito and James R. Martin II. *J. Geotech. Geoenviron. Eng.* **2003**, *129*, 387–389. [CrossRef]
40. Tao, M.; Fugueroa, J.L.; Saada, A.S. Influence of Nonplastic Fines Content on the Liquefaction Resistance of Soils in Terms of the Unit Energy. In *Cyclic Behaviour of Soils and Liquefaction Phenomena*; CRC Press: Boca Raton, FL, USA, 2004; pp. 223–231.
41. Yang, S. Characterization of the Properties of Sand-Silt Mixtures. Ph.D. Thesis, Norwegian University of Science and Technology, Trondheim, Norway, 2004.
42. Chang, C.S.; Deng, Y. Revisiting the Concept of Inter-Granular Void Ratio in View of Particle Packing Theory. *Géotechnique Lett.* **2019**, *9*, 121–129. [CrossRef]
43. Han, D.; Nur, A.; Morgan, D. Effects of Porosity and Clay Content on Wave Velocities in Sandstones. *Geophysics* **1986**, *51*, 2093–2107. [CrossRef]